

Birthe Stüven^a, Robert Stabel^a, Robert Ohlendorf^b, Julian Beck, Roman Schubert and Andreas Möglich^{*}

Characterization and engineering of photoactivated adenylyl cyclases

<https://doi.org/10.1515/hsz-2018-0375>

Received September 15, 2018; accepted December 7, 2018; previously published online December 14, 2018

Abstract: Cyclic nucleoside monophosphates (cNMP) serve as universal second messengers in signal transduction across prokaryotes and eukaryotes. As signaling often relies on transiently formed microdomains of elevated second messenger concentration, means to precisely perturb the spatiotemporal dynamics of cNMPs are uniquely poised for the interrogation of the underlying physiological processes. Optogenetics appears particularly suited as it affords light-dependent, accurate control in time and space of diverse cellular processes. Several sensory photoreceptors function as photoactivated adenylyl cyclases (PAC) and hence serve as light-regulated actuators for the control of intracellular levels of 3', 5'-cyclic adenosine monophosphate. To characterize PACs and to refine their properties, we devised a test bed for the facile analysis of these photoreceptors. Cyclase activity is monitored in bacterial cells via expression of a fluorescent reporter, and programmable illumination allows the rapid exploration of multiple lighting regimes. We thus probed two PACs responding to blue and red light, respectively, and observed significant dark activity for both. We next engineered derivatives of the red-light-sensitive PAC with altered responses to light, with one variant, denoted *DdPAC*, showing enhanced

response to light. These PAC variants stand to enrich the optogenetic toolkit and thus facilitate the detailed analysis of cNMP metabolism and signaling.

Keywords: adenylyl cyclase; BLUF; optogenetics; phytochrome; sensory photoreceptor; synthetic biology.

Introduction

Second messenger molecules are integral to signal-transduction networks across most organisms. As intracellular, diffusible agents, they amplify and relay signals in time and space within cells (Krauss, 2014). As one class of universal second messengers, 3', 5'-cyclic nucleoside monophosphates (cNMP) are engaged in regulating manifold physiological processes in prokaryotes and eukaryotes alike. cNMPs are generally produced from the corresponding 5'-nucleoside triphosphates by nucleotidyl cyclases and are degraded to the non-cyclic 5'-nucleoside monophosphates by phosphodiesterases (PDE). In eukaryotic cells, the two predominant cNMPs, 3', 5'-cyclic adenosine monophosphate (cAMP) and 3', 5'-cyclic guanosine monophosphate (cGMP) (Rall et al., 1957; Ashman et al., 1963), bind to and thereby modulate the activity of multiple targets, including protein kinases A and G (Walsh et al., 1968; Kuo and Greengard, 1970), cyclic-nucleotide-gated (CNG) ion channels (Fesenko et al., 1985), Epac (exchange protein directly activated by cAMP) (de Rooij et al., 1998), and popeye-domain-containing proteins (Andrée et al., 2000). As these cyclic nucleotides play crucial roles in diverse signaling pathways, misregulation of their metabolism can be causative for disease (Gold et al., 2013). In bacteria, cAMP mediates various responses via binding to proteins of the cAMP-receptor protein family (McDonough and Rodriguez, 2012). A particularly well-studied example is the carbon catabolite repression present in most bacteria (Görke and Stülke, 2008). In the presence of their preferred carbon sources, bacteria grow rapidly, and the activity of the endogenous adenylyl cyclase (AC) is inhibited. Once the preferred carbon source is depleted, AC activity ramps up, and intracellular cAMP accumulates. In *Escherichia coli* and related bacteria, cAMP forms a complex with the

^a**Birthe Stüven and Robert Stabel:** These authors contributed equally to this work.

^bPresent address: Department of Biological Engineering, Massachusetts Institute of Technology, Cambridge, MA 02139, USA.

***Corresponding author: Andreas Möglich,** Lehrstuhl für Biochemie, Universität Bayreuth, D-95447 Bayreuth, Germany; Institut für Biologie, Humboldt-Universität zu Berlin, D-10115 Berlin, Germany; Research Center for Bio-Macromolecules, Universität Bayreuth, D-95447 Bayreuth, Germany; Bayreuth Center for Biochemistry and Molecular Biology, Universität Bayreuth, D-95447 Bayreuth, Germany; and North-Bavarian NMR Center, Universität Bayreuth, D-95447 Bayreuth, Germany, e-mail: andreas.moeglich@uni-bayreuth.de.

<https://orcid.org/0000-0002-7382-2772>

Birthe Stüven, Robert Stabel and Julian Beck: Lehrstuhl für Biochemie, Universität Bayreuth, D-95447 Bayreuth, Germany
Robert Ohlendorf and Roman Schubert: Institut für Biologie, Humboldt-Universität zu Berlin, D-10115 Berlin, Germany

catabolite activator protein [CAP, also known as cAMP receptor protein (CRP)] which then binds to the promoter region of numerous target genes and thereby either activates or represses their expression (Shimada et al., 2011). By contrast, cGMP signaling is absent from most bacteria but occurs in certain species (Gomelsky, 2011). As a case in point, the α -proteobacterium *Rhodospirillum centenum* employs a CAP variant that responds to cGMP rather than cAMP (Marden et al., 2011; Roychowdhury et al., 2015). In addition to cNMPs, bacteria also use cyclic dinucleotides as second messengers as exemplified by cyclic diguanylate that is involved in the regulation of manifold processes including cell cycle, biofilm formation and virulence (Jenal et al., 2017).

Signaling pathways relying on cNMPs frequently involve the formation of spatiotemporal microdomains of elevated second messenger concentration. Hence, implements that allow to monitor and alter intracellular cNMP levels with precision in time and space are uniquely suited to investigate and control such pathways. Optogenetics represents a particularly versatile approach as it enables the noninvasive, spatiotemporally precise and reversible perturbation of cellular events by light (Deisseroth et al., 2006). Originating in the neurosciences, optogenetics now extends to manifold cellular processes and parameters including cNMP signaling (Losi et al., 2018). Sensory photoreceptor proteins underpin optogenetics as genetically encodable, light-regulated actuators (Möglich et al., 2010). Several photoreceptors found in nature function as photoactivated adenylyl cyclases (PAC) or guanylyl cyclases that increase production of the respective cNMP upon light exposure. The first discovered PAC from the protist *Euglena gracilis* (Iseki et al., 2002), denoted *EuPAC*, responds to blue light through a flavin-binding BLUF photosensor module (Gomelsky and Klug, 2002). Although *EuPAC* has seen optogenetic use (Schröder-Lang et al., 2007), it has been largely superseded by *bPAC* from the γ -proteobacterium *Beggiatoa* sp. which offers smaller and simpler protein architecture combined with more pronounced blue-light-dependent regulation of AC activity compared to *EuPAC* (Ryu et al., 2010; Stierl et al., 2011). *bPAC* has thus become a tool of choice in optogenetics (Jansen et al., 2017), and variants have been engineered that possess guanylyl cyclase (GC) activity (Ryu et al., 2010; Kim et al., 2015). Other naturally occurring photoactivated nucleotidyl cyclases resort to light-oxygen-voltage, rhodopsin and cyanobacteriochrome photosensor units (Rafaelberg et al., 2013; Avelar et al., 2014; Blain-Hartung et al., 2018). Striving to extend the light sensitivity of PACs to the long-wavelength spectral range, Gomelsky and colleagues engineered the red-light-regulated AC *IlaC* by fusing the

photosensory core module (PCM), comprising PAS, GAF and PHY domains, of the *Rhodobacter sphaeroides* bacteriophytochrome (BPhy) BPhG1 to the catalytic effector module of the *Nostoc* sp. AC CyaB1 (Ryu et al., 2014). Notably, BPhys utilize the linear tetrapyrrole biliverdin as chromophore and adopt two (meta)stable states, denoted Pr and Pfr. Absorption of red and far-red light drive the Pr \rightarrow Pfr and Pfr \rightarrow Pr transitions, respectively (Rockwell and Lagarias, 2010). Recently, Winkler and colleagues refined this engineering approach and fused the *Deinococcus radiodurans* BPhy (*DrBPhy*) PCM to the effector module of *Synechocystis* PCC6803 Cya2 (Ettl et al., 2018) to obtain the red-light-regulated GC PaaG. Via introduction of a previously described single-residue substitution within the effector module (Rauch et al., 2008), PaaG was converted to a PAC named PaaC (Ettl et al., 2018). In a similar vein, we generated the red-light-activated cAMP- and cGMP-specific PDE LAPD by recombining the *DrBPhy* PCM with the effector module of *Homo sapiens* PDE2A (Gasser et al., 2014).

The mechanistic characterization and optimization of photoactivated cyclases and phosphodiesterases require efficient assays that probe enzymatic activity under different lighting conditions. Formation and breakdown of cNMPs can be routinely quantified by high-performance liquid chromatography (HPLC). While highly precise and well suited for recording complete Michaelis-Menten kinetics, HPLC-based assays usually necessitate prior purification of the enzymes which may prove limiting when studying large numbers of variants, e.g. en route to the development of optimized light-regulated enzymes. Several assays overcome this limitation by doing away with protein purification. Enzyme-linked immunosorbent assays (ELISAs) are capable of precisely determining cNMP quantities even within heterogenous mixtures like cell lysates. Similarly, we developed a fluorescence-based readout that exploits that both the making and the breaking of cNMPs entail acidification of the solution (Schumacher et al., 2016). Cyclase and PDE turnover can hence be detected via the pH-sensitive fluorophore 2',7'-bis-(2-carboxyethyl)-5-(and-6)-carboxyfluorescein (BCECF) (Rink et al., 1982), and this assay applies to either purified protein or crude cell lysates, thus allowing enhanced throughput. Finally, approaches exist that permit the detection of light-regulated cyclase activity inside of bacterial cells. One of the targets in *E. coli* upregulated via action of CAP:cAMP is the *lac* operon which encodes genes engaged in metabolizing lactose. Intracellular cAMP levels can hence be indirectly detected by monitoring the activity of gene products of this operon, in particular of β -galactosidase (LacZ) which is essential for hydrolytic

breakdown of lactose and subsequent metabolization. In one approach, bacterial growth on minimal medium containing lactose as sole carbon source is monitored, often combined with a pH-indicator dye (so-called MacConkey agar) (Ryu et al., 2010). Alternatively, the enzymatic activity of LacZ is assessed via lactose analogs, such as X-gal, that upon hydrolysis yield colored output (Ryu et al., 2014, 2015; Etzl et al., 2018). For tests in eukaryotic cells, PACs were combined with CNG channels, thus allowing readout of activity via electrophysiology or ion-sensitive fluorophores (Stierl et al., 2011; Jansen et al., 2015).

In the present work, we strove to analyze and optimize the performance of PACs. To this end, we devised a bacterial assay that reports on intracellular AC activity and affords sensitive fluorescent readout. The reporter assay seamlessly integrates with a setup for the programmable illumination of microtiter plates (MTP), thus affording the facile, parallelized interrogation of multiple experimental conditions and lighting regimes. The resulting test bed readily recorded light-dependent readout for both bPAC and PaaC. Thus equipped, we engineered PaaC

derivatives that differ in their activation profiles, with one variant offering the advantage of reduced sensitivity to far-red light compared to PaaC.

Results

A test bed for photoactivated adenylyl cyclases

To streamline the characterization and optimization of photoactivated adenylyl cyclases, we devised an efficient screening platform. We reasoned that an ideal platform would possess key desirable traits: (i) the readout of catalytic activity should be specific and sensitive; (ii) the readout should be facile, ideally obviating laborious purification of candidate cyclases; (iii) the readout should be compatible with various illumination regimes and should avoid undue photoactivation of the system under study; (iv) the platform should be scalable and parallelizable

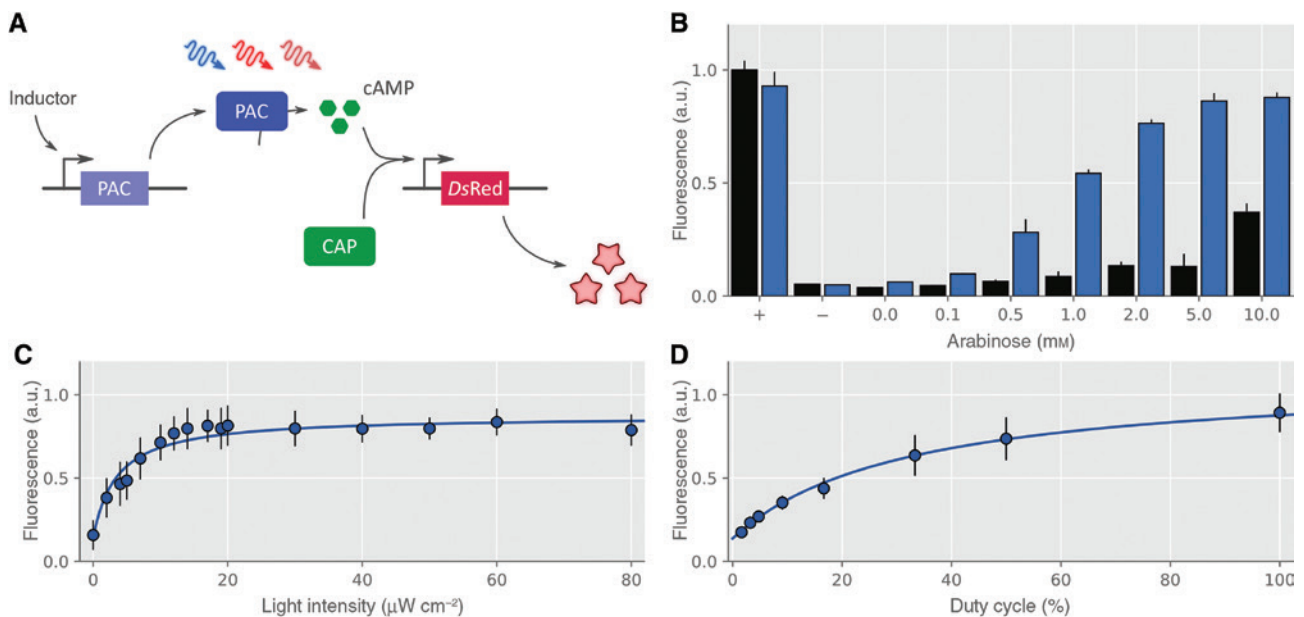


Figure 1: Test bed for photoactivated adenylyl cyclases (PAC) as applied to bPAC.

(A) A reporter-gene assay for PACs was realized in the *E. coli* strain CmpX13 $\Delta cyaA$ on two plasmids. The first plasmid harbors a PAC gene cassette, the expression of which is controlled by inducer addition. Once functionally expressed, the PAC enzyme catalyzes the production of intracellular 3', 5'-cyclic adenosine monophosphate (cAMP) depending upon illumination. cAMP binds to the endogenous catabolite activator protein (CAP) and the resultant CAP:cAMP complex induces expression of the red-fluorescent reporter *DsRed* from the second plasmid denoted pCyclR. (B) *DsRed* reporter-gene activity for cultures expressing bPAC at different strength as controlled by L-arabinose addition. Readings for cultures incubated in darkness or under 40 $\mu\text{W cm}^{-2}$ 470-nm light are shown in black and blue, respectively. Cultures expressing CyaA instead of bPAC or carrying an empty expression vector serve as a positive and negative controls (indicated by the + and - signs). Fluorescence data were normalized to optical density of cultures and represent mean \pm SD of four biological replicates. (C) Expression of bPAC was induced with 5 mM L-arabinose, and reporter-gene activity recorded at different intensities of continuous 470-nm illumination. (D) The response of bPAC, induced by 5 mM L-arabinose, to pulsed illumination of 470 nm and 40 $\mu\text{W cm}^{-2}$ intensity was assessed.

to afford the interrogation of manifold cyclase variants and lighting regimes (color, intensity, duration, pulsed light). To meet these criteria, we envisioned a bacterial reporter assay based on the cAMP-dependent expression of a red-fluorescent reporter (Figure 1A). Intracellular, light-dependent cyclase activity could hence be linked to a stable readout which can be recorded in intact cells and is both sensitive and specific (criteria i and ii). Provided the fluorescence reporter persists over time, illumination of the system and readout can be temporally separated, and cross-talk thereby largely minimized (criterion iii). Lastly, fluorescence readout is compatible with many assay formats and can be detected with even single-cell sensitivity (criterion iv). To implement this system, we opted for the *E. coli lac* promoter which is intrinsically weak but comprises a binding site for the catabolite activator protein (Malan and McClure, 1984). Binding of the CAP:cAMP complex to this operator site strongly upregulates expression of downstream genes. We constructed the plasmid pCyclR in which this promoter controls expression of the *DsRed Express2* reporter (Strack et al., 2008), a stable, well-tolerated fluorescent protein suitable for whole-cell labeling (Ohlendorf et al., 2012; Richter et al., 2016). We first assessed the performance of this reporter system in the *E. coli* strain CmpX13 (Mathes et al., 2009) which is a BL21 derivative stably expressing a riboflavin transporter. Upon over-night cultivation at 37°C, CmpX13 cultures harboring pCyclR exhibited intense *DsRed* fluorescence, indicative of strong promoter activity even in the absence of any photoactivated adenylyl cyclase. To reduce background activation of the *lac* promoter, we generated a knockout strain in which the endogenous *E. coli* adenylyl cyclase CyaA is disrupted. In the resultant CmpX13 $\Delta cyaA$ strain, the pCyclR reporter only yielded ~50-fold reduced, low fluorescence (Figure 1B; negative control). When CyaA was ectopically expressed from an additional medium-copy pBAD plasmid with pBR322 origin of replication, high fluorescence readout was restored, thus confirming principal functionality of the cAMP reporter assay. All subsequent experiments were carried out in the CmpX13 $\Delta cyaA$ strain.

To calibrate the system, we next replaced the CyaA cyclase in the pBAD plasmid with the photoactivated adenylyl cyclase bPAC that is sensitive to blue light. Upon introduction of this plasmid into the CmpX13 $\Delta cyaA$ pCyclR context, reporter fluorescence increased depending upon bPAC expression strength which was adjusted via addition of up to 10 mM of the inductor L-arabinose (Figure 1B). In the regime of strong expression, elevated reporter fluorescence developed even when cultures were incubated in darkness which is consistent with the substantial dark-state activity reported for bPAC (Ryu et al.,

2010; Stierl et al., 2011) that exceeds that found in certain rhodopsin-coupled cyclases (Avelar et al., 2014; Gao et al., 2015; Scheib et al., 2015). To facilitate characterization of the system response to blue light, the cAMP reporter assay was implemented in 96-well microtiter-plate format. We could thus resort to a programmable matrix of light-emitting diodes (LED) for the illumination of MTPs that we recently reported (Hennemann et al., 2018). Briefly, this setup uses an Arduino open-electronics circuit board to individually control an eight-by-eight array of three-color LEDs with peak wavelengths of 470, 525, and 620 nm. We deployed this setup to assess the response of bPAC within the reporter context to constant illumination at 40 $\mu\text{W cm}^{-2}$ blue light (470 nm) at different concentrations of the inductor L-arabinose. For all inductor amounts greater than zero, *DsRed* reporter fluorescence was elevated under blue light relative to darkness, with the most pronounced difference of ~4.4-fold observed for 5 mM L-arabinose. We note that considerably larger light:dark differences in activity above 100-fold were reported for bPAC when analyzed by high-performance liquid chromatography (HPLC) (Ryu et al., 2010; Stierl et al., 2011). The comparatively diminished difference in our reporter assay is likely due to leakiness of the *lac* promoter, background fluorescence and potentially to non-linearities in the system response, e.g. caused by cooperative reaction steps. That notwithstanding, the cAMP reporter assay qualitatively replicates previous findings for bPAC and hence is suited to characterize the performance of this photoreceptor inside bacterial cells. We repeated the experiment at 5 mM arabinose for different intensities of constant blue-light illumination (Figure 1C). The *DsRed* reporter fluorescence increased hyperbolically with intensity, and a half-maximal dose of $(3.8 \pm 0.8) \mu\text{W cm}^{-2}$ was obtained. Notably, a much higher half-maximal dose of $(3.7 \pm 0.4) \mu\text{W mm}^{-2}$ was determined for the light-induced activation of purified bPAC protein (Stierl et al., 2011). Likewise, in our own measurements, the half-maximal dose for bPAC activation in a coupled reporter assay within mammalian cells amounted to $(5.8 \pm 0.1) \mu\text{W mm}^{-2}$ (Richter et al., 2015). We note that both these earlier measurements reported on acute bPAC activity whereas our current assay integrates bPAC activity over an extended period. Although the underlying reasons remain unclear, these differences between the assays may underpin the observed discrepancy in half-maximal dose for bPAC activation. We next assessed the effect of intermittently applied illumination which can enable multiplexing of several light-responsive circuits and reduce overall required light dose (Hennemann et al., 2018) (Figure 1D). To this end, bacterial cultures were periodically illuminated by blue-light pulses of 40 $\mu\text{W cm}^{-2}$

intensity and 1 min duration followed by dark periods of 0–60 min. Reporter fluorescence increased as a function of duty cycle (defined as the fraction of time during which illumination was applied) with a half-maximal duty cycle of $(32 \pm 6)\%$.

Characterization of red-light-regulated adenylyl cyclases

Having established an efficient test bed for photoactivated adenylyl cyclases, we sought to extend our analysis to other PACs. Variants deriving from the fusion of bacteriophytochrome photosensors with cyclase effector domains (Ryu et al., 2014; Ettl et al., 2018) are regulated by red and far-red light and are of prime interest for at least two principal reasons. First, BPhys are photochromic in that red and far-red light drive the bidirectional transition between the two (meta)stable states Pr and Pfr, thus potentially enabling enhanced precision in space and time (Ziegler and Möglich, 2015). Second, light of longer wavelengths exhibits deeper penetration in tissue which is of particular relevance for *in vivo* optogenetics (Shu et al., 2009). Although our original programmable LED setup can also emit red light (at ~ 620 nm), a far-red option is missing (Hennemann et al., 2018). We hence designed a new programmable, dual-color LED matrix that allows the use of custom LEDs, including such that emit in the red and far-red spectral range. As illustrated in Figure 2, we outfitted the matrix with two sets of 64 LEDs with emission wavelengths of (655 ± 10) and (850 ± 21) nm, respectively, the intensity and timing

of which can be programmed. Thus equipped, we analyzed the red-light-regulated PAC PaaC in the pCyclR reporter-gene setup. To this end, we cloned the *PaaC* gene into a medium-copy pCDF plasmid that also harbors an expression cassette for *Synechocystis* sp. heme oxygenase 1 (SsHO1), an enzyme which provides the biliverdin chromophore via oxidative cleavage of heme. The expression of both PaaC and SsHO1 from this plasmid can be adjusted via addition of the inductor isopropyl β -D-1-thiogalactopyranoside (IPTG). We introduced the plasmid into the CmpX13 Δ *cyaA* pCyclR context and measured reporter readout after incubation in darkness or under constant illumination with 655 or 850 nm at $40 \mu\text{W cm}^{-2}$ intensity (Figure 3A). For samples incubated in darkness, low *DsRed* fluorescence was obtained that only slightly increased with inductor concentration. For the cultures grown under 655-nm light, *DsRed* fluorescence was elevated relative to the dark-incubated samples, with a maximally 9-fold upregulation at 1 mM IPTG. Unexpectedly, illumination with 850 nm also prompted an increase in reporter fluorescence to around 40% of the values observed for illumination with 655 nm. Although the peak wavelength of the LED at 850 nm is well separated from the absorption spectrum of the Pr state of the *DrBPhy* photosensor (Figure 4A), evidently the short-wavelength tail of the emission spectrum suffices for actuating PaaC. To arrive at a better understanding of this effect, we reran the experiment at a constant inductor concentration of 1 mM but varying intensities of constant illumination with either 655 nm or 850 nm (Figure 3B). For both light qualities, *DsRed* reporter fluorescence hyperbolically increased with intensity and displayed half-maximal

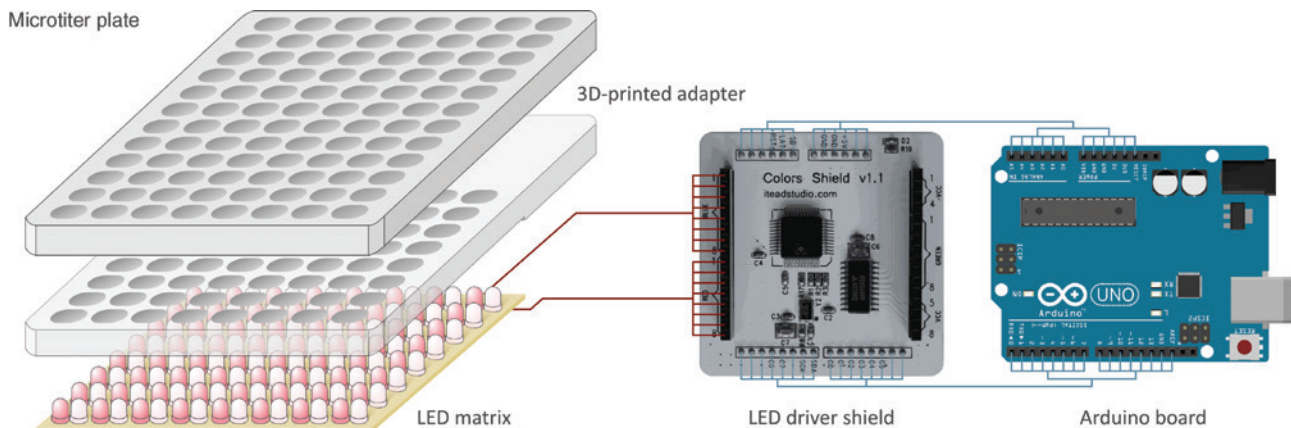


Figure 2: Schematic of a programmable matrix of light-emitting diodes (LED) for the illumination of microtiter plates (MTP). A circuit board was outfitted with two sets of 64 LEDs with peak emission wavelengths of 655 and 850 nm. A 3D-printed adapter encases this board and enables the illumination from below of 64 wells of an MTP with one 655-nm and one 850-nm LED per well. Timing and intensity of the LEDs can be individually configured via a driver shield that is controlled by a conventional Arduino board. Programming of the LED matrix is facilitated by a graphical user interface implemented in Python.

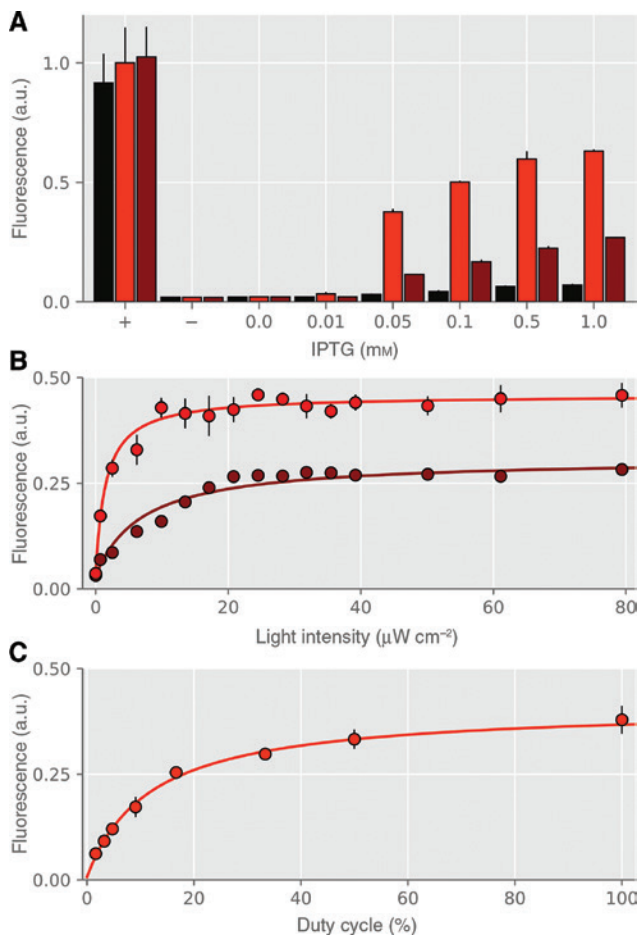


Figure 3: Reporter-gene assay for PaaC.

(A) Expression of PaaC was induced by IPTG addition and *DsRed* reporter readout recorded for cultures grown in darkness (black) or under constant illumination with 655 nm (red) or 850 nm (brown). *CyaA* positive and empty-vector negative controls are denoted by + and – signs. (B) Reporter-gene activity for PaaC, induced with 0.05 mM IPTG, under constant illumination with 655- and 850-nm light of different intensities. (C) Reporter readout for application of intermittent 655-nm light at $40 \mu\text{W cm}^{-2}$ intensity.

doses of (2.0 ± 0.4) and $(7.0 \pm 1.6) \mu\text{W cm}^{-2}$, respectively. The observation that near-infrared light activates PaaC to considerable extent is reminiscent of the red-light-activated phosphodiesterase LAPD which is also based on the *DrBPhy* photosensor (Gasser et al., 2014). In this system, red light prompted an increase of catalytic activity that could only be partially reverted by near-infrared light. In marked contrast to the present findings for PaaC, illumination of dark-adapted LAPD with 850 nm did not upregulate catalytic activity. We also subjected the PaaC-expressing cultures to intermittent illumination with 655 nm at $40 \mu\text{W cm}^{-2}$ and found that *DsRed* reporter fluorescence increased with a half-maximal duty cycle of $(12 \pm 2)\%$ (Figure 3C).

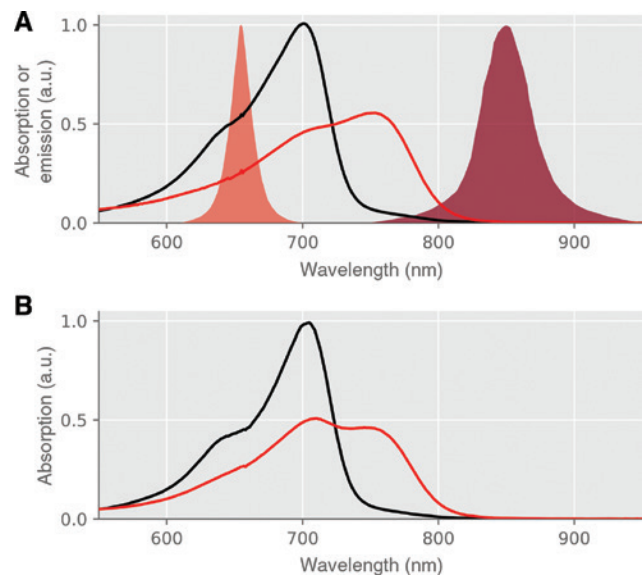


Figure 4: Absorption spectra of bacteriophytochrome proteins and emission spectra of LEDs used in programmable matrix. (A) The absorption spectra of the PAS-GAF-PHY PCM from *D. radiodurans* following saturating illumination with red and far-red light, respectively, are drawn as red and black lines. The emission spectra of the 655-nm and 855-nm LEDs are shown as shaded areas in red and brown. (B) The absorption spectra of the PCM from *D. deserti* following saturating illumination with red and far-red light, respectively, are drawn as red and black lines.

Engineering red-light-regulated adenylyl cyclases

We next addressed whether the design blueprint underpinning PaaC developed by the Winkler group (Ettl et al., 2018) and based on pioneering work by the Gomelsky laboratory (Ryu et al., 2014) extends to other BPhys photosensors. Put another way, is it possible to construct additional red-light-sensitive PACs according to the same rationale, and if so, do the resultant photoreceptors differ in their properties? In addressing these questions, we capitalized on the test bed that we implemented for light-regulated adenylyl cyclases. We replaced the *DrBPhy* photosensor module in PaaC by the homologous PCM segments of the BPhys from *Deinococcus deserti* (*DdBPhy*), *Pseudomonas aeruginosa* (*PaBPhy*) and *Janthinobacter CG23_2* (*JaBPhy*). As the length of the linker between photosensor and effector moieties can greatly alter activity and regulation by light of photoreceptors (Möglich et al., 2009; Gasser et al., 2014; Ryu et al., 2014; Ettl et al., 2018), we retained the linker length used in PaaC (Figure 5). The choice of the specific BPhys was motivated by the close homology between *DdBPhy* and *DrBPhy*, and by *PaBPhy* being a bathy-bacteriophytochrome (Yang et al., 2008)

		← BPhy	Cya2 →
PaaC	461	DDLGP [↓] RHSFDTYLEEKRGYAE [↓] PWHHPGEIEEAQDLRDTLTGALGERLSVIR	VRNTFGRYLTD
DdPAC	465	VDLTPRASFEAYVQQRHTALPWHHPGEVAEAE [↓] SMRDALVETTSVRLTALQ	VRNTFGRYLTD
PaPAC	452	PRLTPRGSFEAWEEVVRGHSTPWSE [↓] TDLAI [↓] AEKLR [↓] LDLMELCLNHAAEVD	VRNTFGRYLTD
JaPAC	463	AQLSPRTSFATWRETITGTSAAWHPGEI [↓] ELATEFRTALLGIALERAEQMA	VRNTFGRYLTD

Figure 5: Sequence alignment of engineered BPhy-cyclases.

The design blueprint PaaC (Ettl et al., 2018) informs the construction of *DdPAC*, *PaPAC* and *JaPAC*. Note that all these BPhy-cyclases are constructed in the same residue register and thus have linkers of the same length between the BPhy photosensor and the adenylyl-cyclase effector modules. The red arrow denotes a residue position that usually is occupied by an aspartate in canonical BPhys (Escobar et al., 2017).

which assumes in its dark-adapted state the Pfr form rather than Pr (Rockwell and Lagarias, 2010). The *JaBPhy* had not been previously characterized in depth but sequence comparisons tentatively assign it as a bathy-BPhy as well; in particular, an aspartate residue within the PHY tongue region prevalent in canonical BPhys is absent from *JaBPhy* (Escobar et al., 2017) (cf. Figure 5, red arrow). As before, we assessed light-regulated cyclase activity in the *CmpX13 ΔcyaA pCyclR* system in either darkness or under illumination with $40 \mu\text{W cm}^{-2}$ 655-nm and 850-nm light. In case of the *DdBPhy*-based variant denoted *DdPAC*, *DsRed* reporter fluorescence for samples incubated under 655-nm light increased with inductor concentration but stayed essentially constant for samples incubated in darkness (Figure 6A). In marked contrast to PaaC, *DdPAC* showed no upregulation of reporter fluorescence with 850-nm light but a slight reduction compared to darkness. The maximum differences between the readout for dark and 655-nm incubation amounted to 9.8-fold, and that between 655-nm and 850-nm illumination to 9.1-fold (Figure 6B). The absorption spectra of the isolated *DdBPhy* PAS-GAF-PHY PCM prior and after red-light illumination closely resembled those obtained for *DrBPhy* (Figure 4B). The variants *PaPAC* and *JaPAC* based on the *bona fide* and putative bathy-BPhys *PaBPhy* and *JaBPhy* showed similar behavior in that reporter readout increased with inductor concentration for all lighting conditions (Figures 7A and 8A). Interestingly, illumination with 655 and 850 nm upregulated *DsRed* fluorescence to the same extent and with similar sensitivity (Figures 7B, C and 8B, C). Taken together, all three PaaC derivatives are genuine PACs with activity that is enhanced by light. The absence of activation by 850-nm light in the *DdPAC* variant might be of advantage for eventual applications in optogenetics, and we thus characterized this protein in more detail. We analyzed cultures, which harbored *DdPAC* and were incubated under varying intensities of 655-nm light and found that *DsRed* fluorescence hyperbolically increased with a half-maximal intensity of $(8.8 \pm 1.6) \mu\text{W cm}^{-2}$, comparable to the value for PaaC. By contrast, no increase in reporter readout was observed

with 855-nm light, even at intensities of up to $80 \mu\text{W cm}^{-2}$ (Figure 6B). Pulsed illumination with 655-nm light enhanced reporter readout with a half-maximal duty cycle of $(26 \pm 4)\%$ (Figure 6C). To determine specific enzymatic activities, we expressed and purified *DdPAC*, and conducted multiple-turnover measurements (Figure 6D). The specific activity for *DdPAC* incubated in darkness or under red light amounted to (8.8 ± 0.1) and $(61.0 \pm 2.8) \cdot 10^{-3}$ mol cAMP (mol enzyme \cdot min) $^{-1}$, respectively, corresponding to a ~ 6.9 -fold difference (Figure 6E). When *DdPAC* was incubated under red light followed by far-red illumination, turnover was decreased to $(8.5 \pm 0.1) \cdot 10^{-3}$ mol cAMP (mol enzyme \cdot min) $^{-1}$, which is around 7.2-fold less than under red light. For comparison, PaaC showed similar overall adenylyl cyclase activity with a 3.8-fold difference between dark-adapted and red-light-exposed enzyme; the influence of subsequent illumination with far-red light was not investigated (Ettl et al., 2018).

Discussion

As evidenced by measurements on two different PAC classes, the reporter setup established in this work provides an efficient test environment for the analysis and optimization of these photoreceptors. By linking light-dependent cyclase activity to bacterial expression of the fluorescent reporter *DsRed*, we achieve sensitive readout that should be compatible with various assay formats and illumination protocols. In contrast to measurements by HPLC, ELISA or BCECF fluorescence (cf. Introduction), our assay reports on AC activity only indirectly, and hence specific enzyme activities cannot be determined. Moreover, as reporter fluorescence is usually evaluated at the end of prolonged incubation and illumination periods, a value that reflects AC activity integrated over time is obtained rather than acute activity readings. In addition, measurements with the cAMP reporter-gene assay will be influenced by the cellular environment and constituents of *E. coli*, not least by the endogenous cAMP-specific PDE CpdA. Notwithstanding these inherent limitations, which

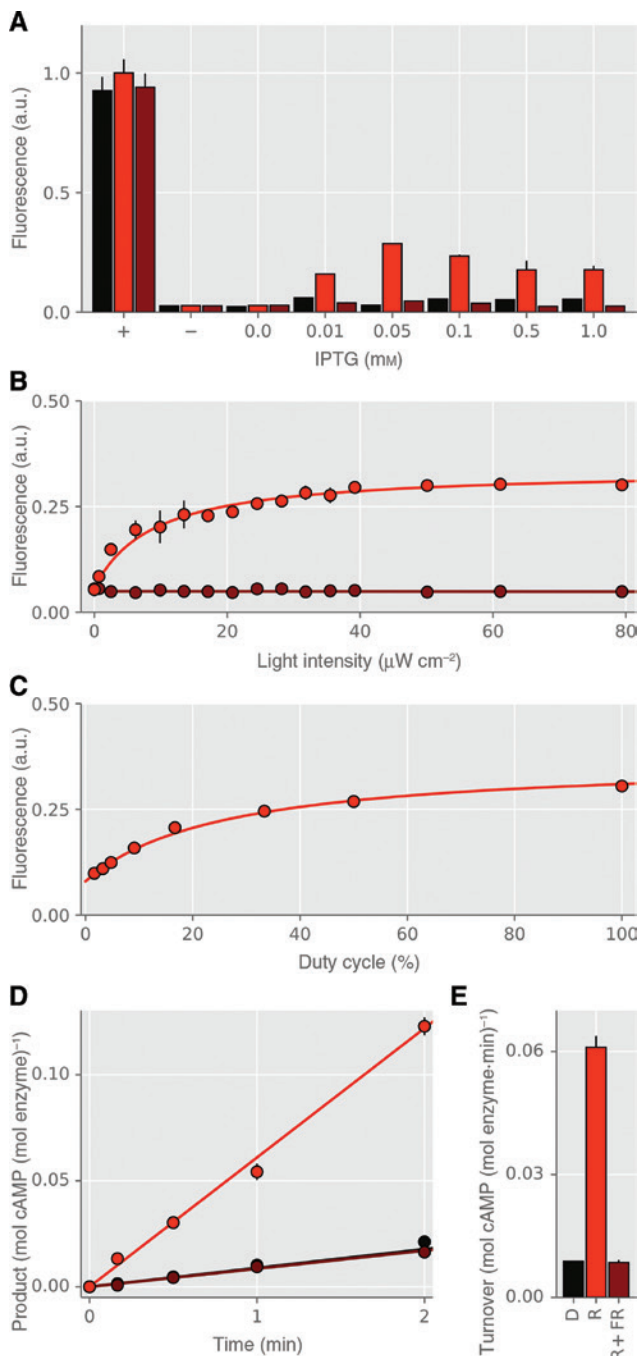


Figure 6: Reporter-gene assay for *DdPAC*.

(A) Expression of *DdPAC* was induced by IPTG addition and *DsRed* reporter readout recorded for cultures grown in darkness (black) or under constant illumination with 655 nm (red) or 850 nm (brown). *CyaA* positive and empty-vector negative controls are denoted by + and – signs, as described in Figure 3. (B) Reporter-gene activity for *DdPAC*, induced with 0.05 mM IPTG, under constant illumination with 655- and 850-nm light of different intensities. (C) Reporter readout for application of intermittent 655-nm light at $40 \mu\text{W cm}^{-2}$ intensity. (D) Adenylyl cyclase activity measured by HPLC for *DdPAC* incubated in darkness (black), under red light (red), or under red light followed by far-red light (brown). (E) Initial reaction velocities from (D).

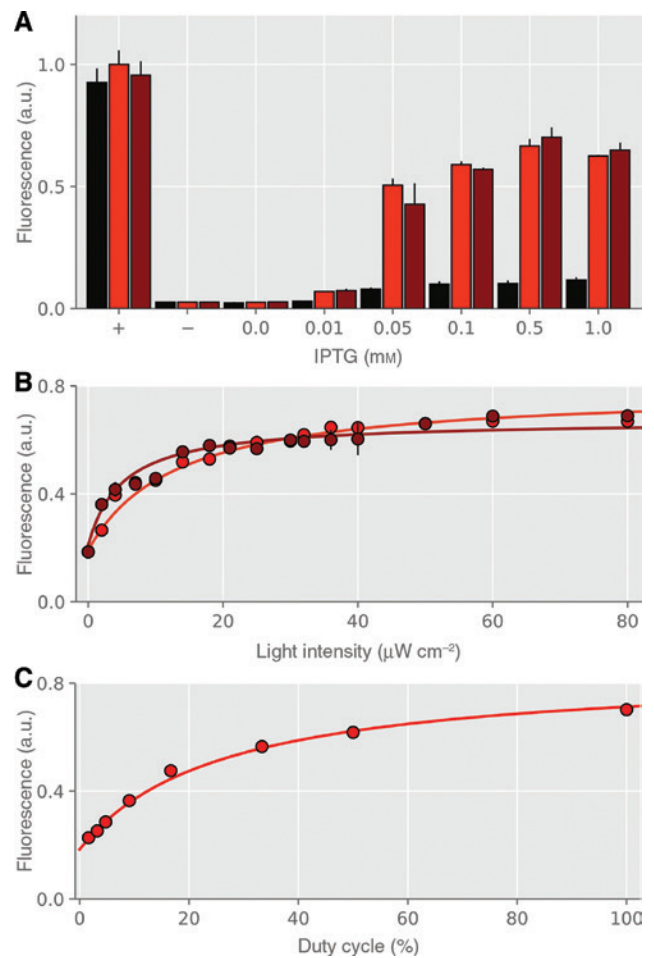


Figure 7: Reporter-gene assay for *PaPAC*.

(A) Expression of *PaPAC* was induced by IPTG addition and *DsRed* reporter readout recorded for cultures grown in darkness (black) or under constant illumination with 655 nm (red) or 850 nm (brown). *CyaA* positive and empty-vector negative controls are denoted by + and – signs, as described in Figure 3. (B) Reporter-gene activity for *PaPAC*, induced with 0.5 mM IPTG, under constant illumination with 655- and 850-nm light of different intensities. (C) Reporter readout for application of intermittent 655-nm light at $40 \mu\text{W cm}^{-2}$ intensity.

also apply to other bacterial assays, e.g. detection via X-gal, the pCyclR setup enables the qualitative characterization of PACs within a cellular setting. The reporter assay lends itself to parallelization and hence to the screening of novel and improved PAC variants. In particular, the fluorescence readout of AC activity enables analysis by flow cytometry and thus facilitates the engineering of enhanced PAC variants via directed evolution and related approaches (Gleichmann et al., 2013).

We combined the facile activity readout afforded by the pCyclR system with custom-built setups for the controllable and parallelizable illumination of samples. Both our previous matrix of light-emitting diodes

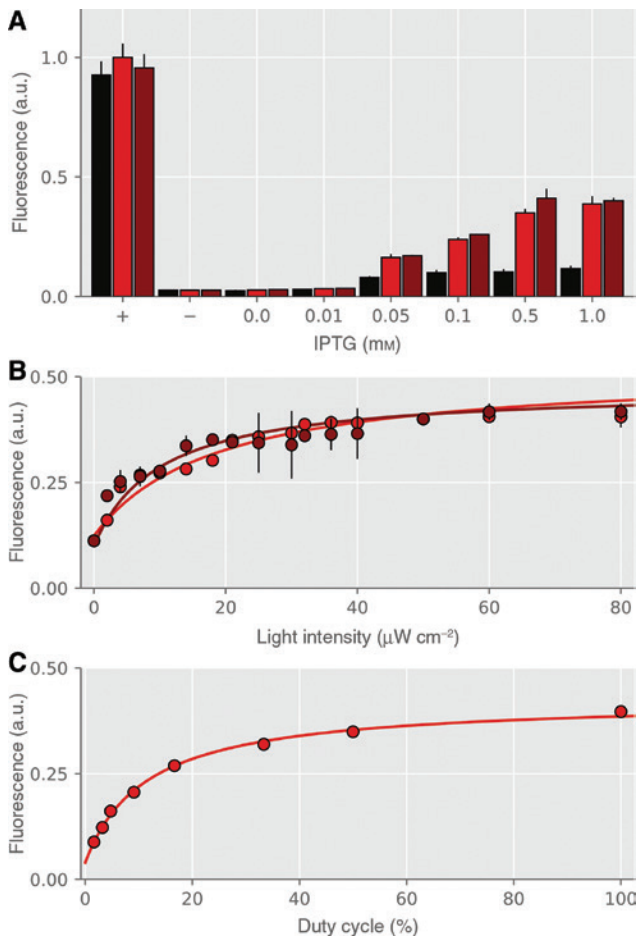


Figure 8: Reporter-gene assay for *JaPAC*.

(A) Expression of *JaPAC* was induced by IPTG addition and *DsRed* reporter readout recorded for cultures grown in darkness (black) or under constant illumination with 655 nm (red) or 850 nm (brown). *CyaA* positive and empty-vector negative controls are denoted by + and – signs, as described in Figure 3. (B) Reporter-gene activity for *JaPAC*, induced with 0.5 mM IPTG, under constant illumination with 655- and 850-nm light of different intensities. (C) Reporter readout for application of intermittent 655-nm light at 40 $\mu\text{W cm}^{-2}$ intensity.

(Hennemann et al., 2018) and the present one are based on open electronics and commercially available, inexpensive parts. Thus, these setups can be readily implemented in most laboratories. The availability of LED matrices of different light color stands to also enable the analysis and optimization of PACs other than *bPAC* and *IlaC*. In particular, the new setup can be equipped with custom LEDs of the required wavelength. An obvious requirement for applying our test bed to other PACs is that they can be functionally expressed in *E. coli* which may for instance prove challenging for the transmembrane rhodopsin-based nucleotidyl cyclases. Currently, our system is restricted to the analysis of AC activity but an extension to measurements of GC activity is conceivable. As remarked

above, certain bacteria possess cGMP-specific CAP variants which might be integrated into our reporter assay. Alternatively, the test environment may be expanded to efficiently screen the activity of cNMP-specific PDEs. More generally, related test and screening platforms could also be established for other second messengers. In particular, bacteriophytochrome photosensors are known to regulate the activity of GGDEF enzymes which catalyze the production of cyclic diguanylate (Ryu and Gomelsky, 2014). Provided a pertinent reporter-gene assay can be built, these enzymes might also be analyzed in efficient manner.

The analysis of *bPAC* and *PaaC* in our test environment revealed residual background activity in darkness, especially in the regime of strong PAC expression. These findings are in line with previous reports on these PACs and indicate scope for improvement. Unexpectedly, *PaaC* was also activated by 850-nm illumination to around half-maximal extent, presumably due to the short-wavelength flank of the LED emission spectrum. Whereas the activation by 655 nm showed a half-maximal dose of $(2.0 \pm 0.4) \mu\text{W cm}^{-2}$, that by 850 nm yielded a value of $(7.0 \pm 1.6) \mu\text{W cm}^{-2}$. Although *PaaC* thus appears more sensitive to 655-nm light, activation by 850-nm light is substantial. These findings indicate that the light-driven $\text{Pfr} \rightarrow \text{Pr}$ transition in *PaaC* is inefficient compared to the $\text{Pr} \rightarrow \text{Pfr}$ transition that entails increase of AC activity. Related observations were made for *LAPD* which shares with *PaaC* the *DrBPhy* PCM; following prior activation of *LAPD* with red light, far-red light could not fully shut off PDE activity (Gasser et al., 2014). It is currently unclear whether these traits of *PaaC* and *LAPD* have the same origin, whether they are rooted in the *DrBPhy* PCM, or whether they are due to the fusion with a heterologous effector module. Detailed biochemical, enzymatic and photochemical analyses will be required to resolve this question.

In the meantime, we have applied our test bed to engineer *PaaC* derivatives that are directly based on the blueprint developed by the Winkler group (Ettl et al., 2018). Strikingly, we succeeded in engineering novel PACs for all three *BPhy* PCMs we tried, suggesting that the design rationale is robust and portable to other photosensors and, by extension, possibly to other effectors. All three PACs presently generated showed light responses that markedly differ from that of *PaaC*. The variants *PaPAC* and *JaPAC* were activated equally well by 655- and 850-nm light. Although this finding implies impairment of the light-driven $\text{Pr} \leftrightarrow \text{Pfr}$ transition, cf. above, these PACs may still be interesting for optogenetic deployment as they are efficiently activated by near-infrared light. As mentioned in the introduction, light of these wavelengths

exhibits superior tissue penetration, and hence these PACs may be attractive for applications *in vivo*. Finally, the *DdPAC* variant differs from *PaaC* by not showing appreciable activation by 850-nm light despite absorption properties of its photosensor module that closely correspond to that of *PaaC* (cf. Figure 4). Measurements of the specific activity showed that *DdPAC* can be effectively switched off by far-red light. Although the underlying reasons for the difference to *PaaC* are unclear, this behavior may indicate improved $Pr \leftrightarrow Pfr$ photoswitching in *DdPAC*. By capitalizing on the PAC test bed presently implemented, *DdPAC* can be readily diversified and thus potentially enhanced. Specifically, the length and composition of the linker between photosensor and effector may be varied. Comparable modifications in the linkers of several engineered, homodimeric photoreceptors modulated activity and regulation by light (Möglich et al., 2009; Gasser et al., 2014; Ryu et al., 2014; Ohlendorf et al., 2016; Ettl et al., 2018). The already existing and upcoming new PAC variants stand to enrich optogenetics and facilitate the precise analysis of manifold processes mediated by cNMPs across diverse organisms.

Materials and methods

Molecular biology

The gene encoding bPAC from *Beggiatoa* sp. was excised from an earlier expression plasmid (Stierl et al., 2011) and cloned into the pBADM-30 vector under control of the arabinose-inducible pBAD promoter by restriction digest with SpeI and HindIII (gift by M. Stierl). Enzymes for molecular biology were obtained from Thermo Fisher Scientific (Dreieich, Germany). As a positive control, the adenylyl cyclase *CyaA* was amplified by PCR from *E. coli* BL21 genomic DNA and cloned into the pBADM-30 plasmid by restriction digest with SpeI and KpnI (primers 5'-GCA CAG ACT AGT TTG TAC CTC TAT ATT GAG AC-3' and 5'-CTG TTG GGT ACC TCA CGA AAA ATA TTG CTG-3'; restriction sites underlined); an empty pBADM-30 vector served as negative control in experiments on bPAC. To construct *PaaC* (Ettl et al., 2018), a gene encoding residues 410–756 of *Cya2* from *Synechocystis* PCC6803 and bearing the E488K substitution (Rauch et al., 2008) was synthesized with *E. coli*-adapted codon usage (GeneArt, Regensburg, Germany). This fragment was then fused to the 3' end of a gene encoding the PCM of *D. radiodurans* BPhy (residues 1–510) via Gibson assembly and cloned (Gibson et al., 2009) into the pCDFDuet vector (Novagen, Darmstadt, Germany) under control of a T7 promoter inducible by IPTG. To aid production of the biliverdin chromophore of BPhys, the *Synechocystis* sp. heme oxygenase 1 gene was additionally placed on the same plasmid under control of T7 and IPTG induction. To this end, the corresponding gene was amplified by PCR from pKT270 (Mukougawa et al., 2006), using the primers 5'-GGA GAT ATA CAT ATG AGT G-3' and 5'-CTA TTC TCG AGC TAG CCT TCG GAG GTG GC-3', and cloned into pCDFDuet by restriction digest with NdeI/XhoI.

A pCDFDuet vector harboring the heme oxygenase but no cyclase gene served as negative control in the experiments. Other BPhy-cyclase variants were cloned by replacing the *DrBPhy* moiety of *PaaC* via Gibson assembly. The gene encoding the PCM of *P. aeruginosa* BPhy (residues 1–501) was amplified from a pET-24a-based vector described in (Yang et al., 2008); genes encoding the PCMs of the *D. deserti* (residues 1–514) and *Janthinobacter* CG23_2 BPhys (residues 1–512) were synthesized with *E. coli* codon adaptation. To construct the pCyclR reporter plasmid, the promoter region in the pET-28c-*DsRed* plasmid (Ohlendorf et al., 2012) was excised with *BglIII/XbaI* and replaced with a promoter fragment of the *lac* operon from *E. coli* BL21 that includes the CAP binding site (nucleotides –84 to +1 relative to the transcription start site).

The Δ *cyaA* knockout variant of the *E. coli* strain CmpX13 (Mathes et al., 2009) was generated according to (Datsenko and Wanner, 2000). Briefly, a kanamycin resistance cassette was amplified by PCR from plasmid pKD4 with the primers 5'-GTT GGC GGA ATC ACA GTC ATG ACG GGT AGC AAA TCA GGC GAT ACG TCT TGG TGT AGG CTG GAG CTG CTT C-3' and 5'-CGG ATA AGC CTC GCT TTC CGG CAC GTT CAT CAC GAA AAA TAT TGC TGT AAC GGC TGA CAT GGG AAT TAG C-3', where the flanking regions homologous to the *E. coli* *cyaA* gene are underlined. The resultant linear PCR fragment was transformed into CmpX13 along with the pKD46 plasmid encoding the λ Red recombinase. Bacteria were selected for genome integration of the cassette by incubation on LB/kanamycin agar. The antibiotic resistance marker was subsequently removed by Flp recombinase encoded on the pCP20 plasmid.

Programmable matrix of light-emitting diodes

For experiments with bPAC, we adapted a previously designed matrix of 8-by-8 individually programmable three-color light-emitting diodes (Hennemann et al., 2018). Briefly, the setup allows the illumination of individual wells of microtiter plates and is realized based on Arduino open electronics and a three-dimensional (3D)-printed housing. A Python/Qt-based graphical user interface allows facile configuration of the LED matrix. In the present revamped design, we adjusted the housing to further minimize light contamination between adjacent wells, and we expanded the Python software to allow the setting of an initial lag period prior to start of illumination. By contrast, the electronics *per se* remained unchanged. Updated versions of the software and template files for the housing are freely available from <http://www.moeglich.uni-bayreuth.de/en/software>.

To achieve programmable illumination of microtiter plates with diverse, customizable LEDs, e.g. red and far-red ones, particularly applicable for experiments with plant and bacterial phytochromes, we reconstructed the programmable LED matrix from scratch. As illustrated in Figure 2, we combined a regular Arduino Uno board with the 'ITEAD Full Color RGB LED Matrix Driver Shield' (Itead, Shenzhen, China). A circuit layout for individually addressing two sets of 8-by-8 LEDs each was designed and printed by the electrical workshop at the University of Bayreuth. We then equipped the circuit board with 64 3-mm 655-nm LEDs [full width at half maximum (fwhm) 20 nm, Kingbright WP908A8SRD] and 64 3-mm 850-nm LEDs (fwhm 42 nm, Harvatek HE1-120AC-XXXX). To fit the new setup, the 3D-printed housing was adjusted accordingly. To allow ready configuration of the revamped setup, we refactored the Python program and the underlying Arduino code but essentially

retained the graphical user interface. A wiring diagram, templates for the circuit board and the housing, and the Python software can be obtained from the mentioned URL. Via the software interface, the light intensities of the LEDs can be adjusted by pulse-width modulation in increments from 0 to 255. The resulting effective light intensities were calibrated with a power meter (model 842-PE, Newport, Darmstadt, Germany) equipped with a silicon photodetector (model 918D-UV-OD3, Newport).

Cyclase reporter-gene assays

The reporter plasmid pCyclR was transformed into chemically competent CmpX13 Δ *cyaA* cells. Empty control vectors (pBADM-30 and pCDFDuet negative controls, cf. above) or plasmids encoding bPAC, various BPhy-cyclases and *E. coli* CyaA (positive control) were additionally introduced into these cells by chemical transformation. Liquid cultures of 5 ml lysogeny broth (LB) supplemented with 50 μ g ml⁻¹ kanamycin (for the pCyclR plasmid) and 50 μ g ml⁻¹ ampicillin (for pBADM-30) or 100 μ g ml⁻¹ streptomycin (for pCDFDuet) were inoculated and grown for 18 h at 37°C. Cultures were then diluted 100-fold in LB (supplemented with antibiotics) and transferred to black-wall clear-bottom 96-well microtiter plates (Greiner BioOne, Frickenhausen, Germany) in a volume of 200 μ l per well. MTPs were sealed with gas-permeable sealing film (BF-400-S, Corning, New York, NY, USA) and incubated for 1 h at 37°C (HN-2 Herp Nursery II, Lucky Reptile, Waldkirch, Germany) and 800 rpm (MTP shaker, PMS-1000i, Grant Instruments, Cambridge, UK). Expression of cyclases was then induced by addition of varying amounts of L-arabinose (for bPAC) or IPTG (for BPhy-cyclases); expression of the positive control CyaA was induced by addition of 10 mM L-arabinose. The incubation of cultures continued for 21 h at 37°C with illumination of the MTP from below via programmable LED arrays, after which the optical density at 600 nm (OD_{600}) and DsRed fluorescence of the bacterial cultures were measured in a Tecan Infinite M200 PRO plate reader (Tecan Group Ltd., Männedorf, Switzerland). For fluorescence detection, excitation and emission wavelengths of (554 \pm 9) nm and (591 \pm 20) nm, respectively, were used. Fluorescence readings were normalized to OD_{600} and are reported as averages of four biological replicates \pm standard deviation (SD), where replicates correspond to separate cultures inoculated from individual bacterial clones. Note that introduction of pCyclR into the CmpX13 Δ *cyaA* strain alone increased fluorescence by around 10-fold compared to the empty bacterial strain. Data were evaluated and plotted with the Fit-o-mat software (Möglich, 2018).

Protein purification and high-performance liquid chromatography

The pCDFDuet plasmid encoding the *Synechocystis* sp. heme oxygenase and DdPAC with a C-terminal His₆ tag (cf. above) was transformed into chemically competent *E. coli* LOBSTR cells (Andersen et al., 2013). Bacteria were grown in LB medium supplemented with 100 μ g ml⁻¹ streptomycin at 37°C and 200 rpm. Upon reaching mid-logarithmic phase (optical density at 600 nm of ~0.6), the bacterial cultures were cooled to 16°C, and 1 mM IPTG and 0.5 mM 5-aminolevulinic acid were added. After incubation for 16 h at 16°C and 200 rpm, cells were harvested and resuspended in lysis buffer [50 mM Tris/HCl pH 8.0, 20 mM NaCl, 20 mM imidazole, complemented with

protease inhibitor mix (Roche, Darmstadt, Germany)]. Lysis was performed via sonication, and the supernatant was applied to a gravity-flow cobalt-sepharose column (HisPur, Thermo Fisher Scientific). Upon washing, the protein was eluted with 200 mM imidazole and dialyzed overnight into 50 mM Tris/HCl pH 8.0, 20 mM NaCl. The protein was further purified by anion-exchange chromatography on a HiTrap Q HP column (Macherey and Nagel, Düren, Germany). Purified protein was dialyzed against storage buffer [50 mM Tris/HCl pH 8.0, 20 mM NaCl, 20% (w/v) glycerol], concentrated, flash-frozen in liquid nitrogen, and stored at -80°C.

Adenylyl cyclase activity of DdPAC was assessed by HPLC as described by (Ettl et al., 2018). To this end, 20 μ M DdPAC was incubated at 20°C in assay buffer (50 mM HEPES pH 7.0, 150 mM NaCl, 50 mM MgCl₂) in the presence of 1 mM substrate ATP. Prior to the measurement, DdPAC was either kept in darkness, or exposed to red light (670 nm, 40 μ W cm⁻², 60 s), or exposed to red light followed by illumination with far-red light (780 nm, 80 μ W cm⁻², 60 s). Reaction aliquots were taken at discrete times, incubated at 95°C for 1 min to stop the reaction, and then cleared by centrifugation for 5 min at 20 000 g. Samples were analyzed on a Kinetex 5u EVO C18 reverse-phase column on a Waters Acquity UPLC using isocratic conditions [20 mM ammonium acetate pH 4.5, 3% (v/v) acetonitrile]. Peak areas were integrated with the Waters Empower software and calibrated against cAMP and ATP standards. All measurements were performed in triplicate.

Acknowledgments: We thank members of the Möglich laboratory for discussions, Dr. Manuela Stierl for providing the pBADM-30-bPAC plasmid, Dr. Tilo Mathes for advice on generating the CmpX13 Δ *cyaA* knockout strain, Norbert Grillenbeck for technical support, and Dr. Markus Lippitz for advice on the design of the LED matrix. We are indebted to the electrical workshop at the University of Bayreuth for circuit-board design and overall stellar support. Funding through Boehringer-Ingelheim Fonds (R.O.), funder id: 10.13039/100005156, a Sofja-Kovalevskaya Award (to A.M.) by the Alexander-von-Humboldt Foundation, and Deutsche Forschungsgemeinschaft (funder id: 10.13039/501100001659, grant MO21921/4-1) is gratefully acknowledged.

References

- Andersen, K.R., Leksa, N.C., and Schwartz, T.U. (2013). Optimized *E. coli* expression strain LOBSTR eliminates common contaminants from His-tag purification. *Proteins Struct. Funct. Bioinform.* **81**, 1857–1861.
- Andrée, B., Hillemann, T., Kessler-Ickelson, G., Schmitt-John, T., Jockusch, H., Arnold, H.-H., and Brand, T. (2000). Isolation and characterization of the novel Popeye gene family expressed in skeletal muscle and heart. *Dev. Biol.* **223**, 371–382.
- Ashman, D.F., Lipton, R., Melicow, M.M., and Price, T.D. (1963). Isolation of adenosine 3', 5'-monophosphate and guanosine 3', 5'-monophosphate from rat urine. *Biochem. Biophys. Res. Commun.* **11**, 330–334.

- Avelar, G.M., Schumacher, R.I., Zaini, P.A., Leonard, G., Richards, T.A., and Gomes, S.L. (2014). A rhodopsin-guanylyl cyclase gene fusion functions in visual perception in a fungus. *Curr. Biol.* *24*, 1234–1240.
- Blain-Hartung, M., Rockwell, N.C., Moreno, M.V., Martin, S.S., Gan, F., Bryant, D.A., and Lagarias, J.C. (2018). Cyanobacteriochrome-based photoswitchable adenylyl cyclases (cPACs) for broad spectrum light regulation of cAMP levels in cells. *J. Biol. Chem.* *293*, 8473–8483.
- Datsenko, K.A. and Wanner, B.L. (2000). One-step inactivation of chromosomal genes in *Escherichia coli* K-12 using PCR products. *Proc. Natl. Acad. Sci. USA* *97*, 6640–6645.
- de Rooij, J., Zwartkruis, F.J.T., Verheijen, M.H.G., Cool, R.H., Nijman, S.M.B., Wittinghofer, A., and Bos, J.L. (1998). Epac is a Rap1 guanine-nucleotide-exchange factor directly activated by cyclic AMP. *Nature* *396*, 474–477.
- Deisseroth, K., Feng, G., Majewska, A.K., Miesenböck, G., Ting, A., and Schnitzer, M.J. (2006). Next-generation optical technologies for illuminating genetically targeted brain circuits. *J. Neurosci.* *26*, 10380–10386.
- Escobar, F.V., Buhrke, D., Michael, N., Sauthof, L., Wilkening, S., Tavraz, N.N., Salewski, J., Frankenberg-Dinkel, N., Mroginski, M.A., Scheerer, P., et al. (2017). Common structural elements in the chromophore binding pocket of the Pfr state of bathy phytochromes. *Photochem. Photobiol.* *93*, 724–732.
- Etzl, S., Lindner, R., Nelson, M.D., and Winkler, A. (2018). Structure-guided design and functional characterization of an artificial red light-regulated guanylate/adenylate cyclase for optogenetic applications. *J. Biol. Chem.* *293*, 9078–9089.
- Fesenko, E.E., Kolesnikov, S.S., and Lyubarsky, A.L. (1985). Induction by cyclic GMP of cationic conductance in plasma membrane of retinal rod outer segment. *Nature* *313*, 310–313.
- Gao, S., Nagpal, J., Schneider, M.W., Kozjak-Pavlovic, V., Nagel, G., and Gottschalk, A. (2015). Optogenetic manipulation of cGMP in cells and animals by the tightly light-regulated guanylyl-cyclase opsin CyclOp. *Nat. Commun.* *6*, 8046.
- Gasser, C., Taiber, S., Yeh, C.-M., Wittig, C.H., Hegemann, P., Ryu, S., Wunder, F., and Möglich, A. (2014). Engineering of a red-light-activated human cAMP/cGMP-specific phosphodiesterase. *Proc. Natl. Acad. Sci. USA* *111*, 8803–8808.
- Gibson, D.G., Young, L., Chuang, R.-Y., Venter, J.C., Hutchison, C.A., and Smith, H.O. (2009). Enzymatic assembly of DNA molecules up to several hundred kilobases. *Nat. Methods* *6*, 343–345.
- Gleichmann, T., Diensthuber, R.P., and Möglich, A. (2013). Charting the signal trajectory in a light-oxygen-voltage photoreceptor by random mutagenesis and covariance analysis. *J. Biol. Chem.* *288*, 29345–29355.
- Gold, M.G., Gonen, T., and Scott, J.D. (2013). Local cAMP signaling in disease at a glance. *J. Cell Sci.* *126*, 4537–4543.
- Gomelsky, M. (2011). cAMP, c-di-GMP, c-di-AMP and now cGMP: bacteria use them all! *Mol. Microbiol.* *79*, 562–565.
- Gomelsky, M. and Klug, G. (2002). BLUF: a novel FAD-binding domain involved in sensory transduction in microorganisms. *Trends Biochem. Sci.* *27*, 497–500.
- Görke, B. and Stülke, J. (2008). Carbon catabolite repression in bacteria: many ways to make the most out of nutrients. *Nat. Rev. Microbiol.* *6*, 613–624.
- Hennemann, J., Iwasaki, R.S., Grund, T.N., Diensthuber, R.P., Richter, F., and Möglich, A. (2018). Optogenetic control by pulsed illumination. *ChemBioChem* *19*, 1296–1304.
- Iseki, M., Matsunaga, S., Murakami, A., Ohno, K., Shiga, K., Yoshida, K., Sugai, M., Takahashi, T., Hori, T., and Watanabe, M. (2002). A blue-light-activated adenylyl cyclase mediates photoavoidance in *Euglena gracilis*. *Nature* *415*, 1047–1051.
- Jansen, V., Alvarez, L., Balbach, M., Strünker, T., Hegemann, P., Kaupp, U.B., and Wachten, D. (2015). Controlling fertilization and cAMP signaling in sperm by optogenetics. *eLife* *4*, e05161.
- Jansen, V., Jikeli, J.F., and Wachten, D. (2017). How to control cyclic nucleotide signaling by light. *Curr. Opin. Biotechnol.* *48*, 15–20.
- Jenal, U., Reinders, A., and Lori, C. (2017). Cyclic di-GMP: second messenger extraordinaire. *Nat. Rev. Microbiol.* *15*, 271–284.
- Kim, T., Folcher, M., Baba, M.D.-E., and Fussenegger, M. (2015). A synthetic erectile optogenetic stimulator enabling blue-light-inducible penile erection. *Angew. Chem. Int. Ed.* *54*, 5933–5938.
- Krauss, G. (2014). *Biochemistry of Signal Transduction and Regulation* (Weinheim, Germany: Wiley-VCH).
- Kuo, J.F. and Greengard, P. (1970). Cyclic nucleotide-dependent protein kinases. VI. Isolation and partial purification of a protein kinase activated by guanosine 3',5'-monophosphate. *J. Biol. Chem.* *245*, 2493–2498.
- Losi, A., Gardner, K.H., and Möglich, A. (2018). Blue-light receptors for optogenetics. *Chem. Rev.* *118*, 10659–10709.
- Malan, T.P. and McClure, W.R. (1984). Dual promoter control of the *Escherichia coli* lactose operon. *Cell* *39*, 173–180.
- Marden, J.N., Dong, Q., Roychowdhury, S., Berleman, J.E., and Bauer, C.E. (2011). Cyclic GMP controls *Rhodospirillum rubrum* cyst development. *Mol. Microbiol.* *79*, 600–615.
- Mathes, T., Vogl, C., Stolz, J., and Hegemann, P. (2009). *In vivo* generation of flavoproteins with modified cofactors. *J. Mol. Biol.* *385*, 1511–1518.
- McDonough, K.A. and Rodriguez, A. (2012). The myriad roles of cyclic AMP in microbial pathogens: from signal to sword. *Nat. Rev. Microbiol.* *10*, 27–38.
- Möglich, A. (2018). An open-source, cross-platform resource for nonlinear least-squares curve fitting. *J. Chem. Educ.* *95*, 2273–2278.
- Möglich, A., Ayers, R.A., and Moffat, K. (2009). Design and signaling mechanism of light-regulated histidine kinases. *J. Mol. Biol.* *385*, 1433–1444.
- Möglich, A., Yang, X., Ayers, R.A., and Moffat, K. (2010). Structure and function of plant photoreceptors. *Annu. Rev. Plant Biol.* *61*, 21–47.
- Mukougawa, K., Kanamoto, H., Kobayashi, T., Yokota, A., and Kohchi, T. (2006). Metabolic engineering to produce phytochromes with phytochromobilin, phycocyanobilin, or phycoerythrobilin chromophore in *Escherichia coli*. *FEBS Lett.* *580*, 1333–1338.
- Ohlendorf, R., Vidavski, R.R., Eldar, A., Moffat, K., and Möglich, A. (2012). From dusk till dawn: one-plasmid systems for light-regulated gene expression. *J. Mol. Biol.* *416*, 534–542.
- Ohlendorf, R., Schumacher, C.H., Richter, F., and Möglich, A. (2016). Library-aided probing of linker determinants in hybrid photoreceptors. *ACS Synth. Biol.* *5*, 1117–1126.
- Raffelberg, S., Wang, L., Gao, S., Losi, A., Gärtner, W., and Nagel, G. (2013). A LOV-domain-mediated blue-light-activated adenylyl cyclase from the cyanobacterium *Microcoleus chthonoplastes* PCC 7420. *Biochem. J.* *455*, 359–365.
- Rall, T.W., Sutherland, E.W., and Berthet, J. (1957). The relationship of epinephrine and glucagon to liver phosphorylase Iv. Effect of epinephrine and glucagon on the reactivation of phosphorylase in liver homogenates. *J. Biol. Chem.* *224*, 463–475.

- Rauch, A., Leipelt, M., Russwurm, M., and Steegborn, C. (2008). Crystal structure of the guanylyl cyclase Cya2. *Proc. Natl. Acad. Sci. USA* 105, 15720–15725.
- Richter, F., Scheib, U.S., Mehlhorn, J., Schubert, R., Wietek, J., Gernezki, O., Hegemann, P., Mathes, T., and Möglich, A. (2015). Upgrading a microplate reader for photobiology and all-optical experiments. *Photochem. Photobiol. Sci.* 14, 270–279.
- Richter, F., Fonfara, I., Bouazza, B., Schumacher, C.H., Bratovič, M., Charpentier, E., and Möglich, A. (2016). Engineering of temperature- and light-switchable Cas9 variants. *Nucleic Acids Res.* 44, 10003–10014.
- Rink, T.J., Tsien, R.Y., and Pozzan, T. (1982). Cytoplasmic pH and free Mg^{2+} in lymphocytes. *J. Cell Biol.* 95, 189–196.
- Rockwell, N.C. and Lagarias, J.C. (2010). A brief history of photochromes. *Chemphyschem Eur. J. Chem. Phys. Phys. Chem.* 11, 1172–1180.
- Roychowdhury, S., Dong, Q., and Bauer, C.E. (2015). DNA-binding properties of a cGMP-binding CRP homologue that controls development of metabolically dormant cysts of *Rhodospirillum rubrum*. *Microbiology* 161, 2256–2264.
- Ryu, M.-H. and Gomelsky, M. (2014). Near-infrared light responsive synthetic c-di-GMP module for optogenetic applications. *ACS Synth. Biol.* 3, 802–810.
- Ryu, M.-H., Moskvina, O.V., Siltberg-Liberles, J., and Gomelsky, M. (2010). Natural and engineered photoactivated nucleotidyl cyclases for optogenetic applications. *J. Biol. Chem.* 285, 41501–41508.
- Ryu, M.-H., Kang, I.-H., Nelson, M.D., Jensen, T.M., Lyuksyutova, A.I., Siltberg-Liberles, J., Raizen, D.M., and Gomelsky, M. (2014). Engineering adenylyl cyclases regulated by near-infrared window light. *Proc. Natl. Acad. Sci. USA* 111, 10167–10172.
- Ryu, M.-H., Youn, H., Kang, I.-H., and Gomelsky, M. (2015). Identification of bacterial guanylate cyclases. *Proteins* 83, 799–804.
- Scheib, U., Stehfest, K., Gee, C.E., Körschen, H.G., Fudim, R., Oertner, T.G., and Hegemann, P. (2015). The rhodopsin–guanylyl cyclase of the aquatic fungus *Blastocladiella emersonii* enables fast optical control of cGMP signaling. *Sci. Signal* 8, rs8.
- Schröder-Lang, S., Schwärzel, M., Seifert, R., Strünker, T., Kateriya, S., Looser, J., Watanabe, M., Kaupp, U.B., Hegemann, P., and Nagel, G. (2007). Fast manipulation of cellular cAMP level by light *in vivo*. *Nat. Methods* 4, 39–42.
- Schumacher, C.H., Körschen, H.G., Nicol, C., Gasser, C., Seifert, R., Schwärzel, M., and Möglich, A. (2016). A fluorometric activity assay for light-regulated cyclic-nucleotide-monophosphate actuators. *Methods Mol. Biol.* 1408, 93–105.
- Shimada, T., Fujita, N., Yamamoto, K., and Ishihama, A. (2011). Novel Roles of cAMP Receptor Protein (CRP) in Regulation of Transport and Metabolism of Carbon Sources. *PLoS One* 6, e20081.
- Shu, X., Royant, A., Lin, M.Z., Aguilera, T.A., Lev-Ram, V., Steinbach, P.A., and Tsien, R.Y. (2009). Mammalian expression of infrared fluorescent proteins engineered from a bacterial phytochrome. *Science* 324, 804–807.
- Stierl, M., Stumpf, P., Udvari, D., Gueta, R., Hagedorn, R., Losi, A., Gärtner, W., Petereit, L., Efetova, M., Schwarzel, M., et al. (2011). Light-modulation of cellular cAMP by a small bacterial photoactivated adenylyl cyclase, bPAC, of the soil bacterium *Beggiatoa*. *J. Biol. Chem.* 286, 1181–1188.
- Strack, R.L., Strongin, D.E., Bhattacharyya, D., Tao, W., Berman, A., Broxmeyer, H.E., Keenan, R.J., and Glick, B.S. (2008). A noncytotoxic DsRed variant for whole-cell labeling. *Nat. Methods* 5, 955–957.
- Walsh, D.A., Perkins, J.P., and Krebs, E.G. (1968). An adenosine 3',5'-monophosphate-dependant protein kinase from rabbit skeletal muscle. *J. Biol. Chem.* 243, 3763–3765.
- Yang, X., Kuk, J., and Moffat, K. (2008). Crystal structure of *Pseudomonas aeruginosa* bacteriophytochrome: Photoconversion and signal transduction. *Proc. Natl. Acad. Sci. USA* 105, 14715–14720.
- Ziegler, T. and Möglich, A. (2015). Photoreceptor engineering. *Front. Mol. Biosci.* 2, 30.